

****FULL TITLE****
*ASP Conference Series, Vol. **VOLUME**, **YEAR OF PUBLICATION***
****NAMES OF EDITORS****

Non-Thermal Radio Emission from Colliding-Wind Binaries

Ronny Blomme

Royal Observatory of Belgium, Ringlaan 3, B-1180 Brussel, Belgium

Abstract. In colliding-wind binaries, shocks accelerate a fraction of the electrons up to relativistic speeds. These electrons then emit synchrotron radiation at radio wavelengths. Whether or not we detect this radiation depends on the size of the free-free absorption region in the stellar winds of both components. One expects long-period binaries to be detectable, but not the short-period ones. It was therefore surprising to find that Cyg OB2 No. 8A ($P = 21.9$ d) does show variability locked with orbital phase.

To investigate this, we developed a model for the relativistic electron generation (including cooling and advection) and the radiative transfer of the synchrotron emission through the stellar wind. Using this model, we show that the synchrotron emitting region in Cyg OB2 No. 8A does extend far enough beyond the free-free absorption region to generate orbit-locked variability in the radio flux.

This model can also be applied to other non-thermal emitters and will prove useful in interpreting observations from future surveys, such as COBRaS – the Cyg OB2 Radio Survey.

1. Introduction

For most hot stars, the radio radiation they emit is due to thermal free-free emission by the ionized material in the stellar wind. A number of stars, however, also show *non-thermal* radio emission, characterized by a negative spectral index¹. This non-thermal emission is believed to be due to electrons that are Fermi-accelerated around shocks (Bell 1978). As these relativistic electrons spiral around in the magnetic field, they emit synchrotron radiation, which we detect as non-thermal radio emission (Bieging et al. 1989). In recent years, it has become clear that the shocks responsible for the Fermi-acceleration in massive stars are those created in the colliding-wind region of a binary (Van Loo et al. 2006, Van Loo, these proceedings).

Non-thermal radio emission from massive stars in general has been reviewed by Benaglia (these proceedings). In the present paper we will be mainly concerned with one specific colliding-wind binary, Cyg OB2 No. 8A. From spectroscopic observations, De Becker et al. (2004, 2006) found it to be an O6If + O5.5III(f) system with a period of 21.908 ± 0.040 d and an eccentricity of 0.24 ± 0.04 . Other parameters relevant for our work are listed in Table 1.

¹The spectral index is given by α , the exponent in the power law relation between flux and frequency: $F_\nu \propto \nu^\alpha$. A stellar wind with a thermal spectrum has $\alpha \approx +0.6$.

Table 1. Parameters of Cyg OB2 No. 8A used in this work. Data from De Becker et al. (2006).

	primary	secondary
T_{eff} (K)	36800	39200
R_* (R_{\odot})	20.0	14.8
M_* (M_{\odot})	44.1	37.4
$\log L_{\text{bol}}/L_{\odot}$	5.82	5.67
\dot{M} ($M_{\odot}\text{yr}^{-1}$)	4.8×10^{-6}	3.0×10^{-6}
v_{∞} (km s^{-1})	1873	2107

This binary has also been known to be a non-thermal radio emitter since the first major survey of O-type star radio emission by Bieging et al. (1989). It was recognized as such by its clearly negative spectral index. The colliding-wind nature of this object is further confirmed by information from its X-ray emission. Observations by De Becker et al. (2006) show an essentially thermal X-ray spectrum, but with an overluminosity of a factor 19-28 compared to the canonical $L_X/L_{\text{bol}} = 10^{-7}$ ratio for O-type stars. This overluminosity is due to additional X-ray emission by material heated in the colliding-wind region. The X-ray light curve also shows variability at the level of $\sim 20\%$. Although the light curve is not well sampled, it suggests that the variability is phase-locked.

Colliding-wind systems such as Cyg OB2 No. 8A are important objects because they can provide information on the Fermi acceleration mechanism, which is also relevant to other fields of astrophysics, such as interplanetary shocks and supernova remnants. The colliding-wind systems can also be used to constrain the amount of clumping and porosity in stellar winds. This is important for mass-loss rate determinations in single stars, which are subject to considerable uncertainties (Puls et al. 2008). Finally, the non-thermal radio emitters can help us detect binaries which are difficult to find spectroscopically and they are therefore useful for improving the determination of the binary frequency in clusters.

2. Radio Variability

Because of the importance of the colliding-wind binary Cyg OB2 No. 8A, we decided to monitor its radio flux. We obtained a number of 6 cm continuum observations with the NRAO² Very Large Array (VLA) during 2005 February 04 to March 12, covering about 1.6 orbital periods. Figure 1 plots these data as a function of phase in the orbital period. The radio fluxes show clear variability and the variability is phase-locked with the orbital period. Furthermore, the data repeat well from one orbit to the next. Since these data were collected,

²The National Radio Astronomy Observatory is a facility of the National Science Foundation operated under cooperative agreement by Associated Universities, Inc.

we have also reduced VLA archive data (Blomme et al. 2009, in preparation). These confirm the phase-locked variability and the orbit to orbit repeatability seen in Fig. 1.

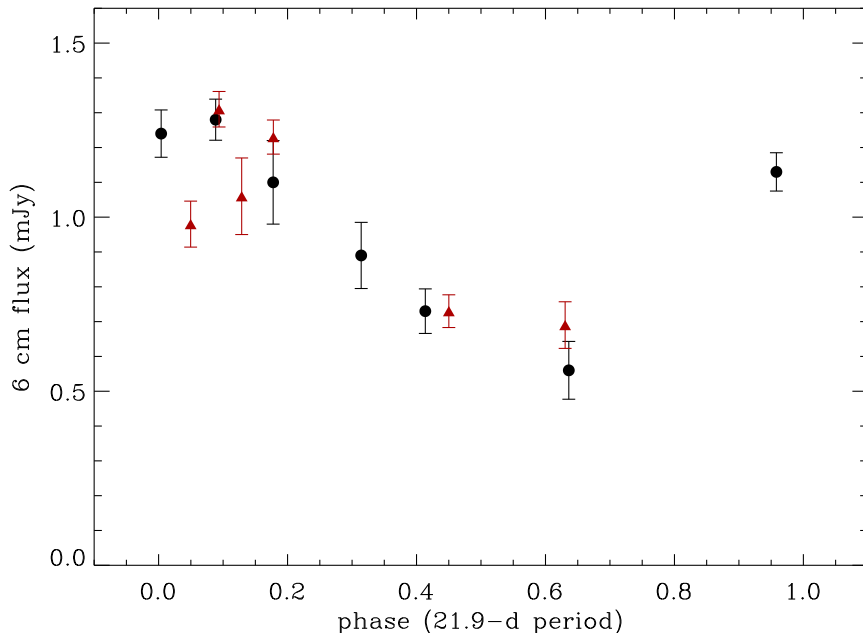


Figure 1. 6 cm radio fluxes of Cyg OB2 No. 8A, as a function of orbital phase. The filled circles indicates data from a first orbit, the filled triangles data from the subsequent orbit.

It is, however, quite surprising that phase-locked variability is found in such a short-period binary. The main part of the colliding-wind region is expected to be comparable in dimension to the separation between the two stars. This size (of order a few stellar radii) is quite small compared to the size of the free-free absorption region of each of the components (of order 100 stellar radii). We therefore expected all the synchrotron emission from the colliding-wind region to be absorbed by the free-free absorption. Hence non-thermal radio emission from Cyg OB2 No. 8A should have been undetectable.

Blomme (2005) made a simple model for this, assuming the synchrotron emission to be a point source positioned between the two stellar components. Following the radiative transfer of the synchrotron emission through the free-free absorption region showed, as expected, no detectable level of non-thermal emission. As the data clearly contradict this, the effect of porosity was also investigated. The porosity variant of the model assumes that the wind is clumped and that at least part of these clumps are optically thick. This allows radiation to escape more easily through the holes between the clumps, allowing us to look deeper into the stellar wind. Porosity models were indeed marginally capable of explaining the fact that we do detect non-thermal radiation from Cyg OB2 No. 8A. This conclusion is important, also in the context of single stars, as

it would help explain the important discrepancies found in the mass-loss rate determinations of massive stars (e.g. Puls et al. 2008).

3. Modelling

The point-source approximation for the synchrotron emitting region is certain to be too simple. We here introduce a more sophisticated model for the colliding-wind region and its associated radio emission. The model does not solve the equations of hydrodynamics. Instead it defines the geometric position of the contact discontinuity between the two winds using the equations from Antokhin et al. (2004). On either side of the contact discontinuity a shock is formed. To simplify the model, we assume that these shocks and the contact discontinuity are at the same geometric place.

At the shocks new relativistic electrons are generated due to the Fermi-acceleration mechanism. Their momenta follow a power-law distribution with a high-energy cut-off due to inverse Compton cooling. The fraction of electrons that become relativistic is determined by assuming that 5% of the shock energy goes into the electron acceleration. We then follow the electrons as they are advected outward along the contact discontinuity. We take into account that they cool down as they do so (due to inverse Compton and adiabatic cooling) and we follow them till they no longer emit synchrotron radiation at the radio wavelengths we are interested in.

Next, we calculate the synchrotron emissivity along the contact discontinuity. We do this in a 2-dimensional model. As the situation is rotationally symmetric around the line connecting the two components, we can then rotate this 2-dimensional emissivity into a 3-dimensional simulation box. Free-free absorption and emission are also added to the model. Finally, we determine the emergent intensity and flux using the radiative transfer technique developed by Adam (1990). We calculate this for a number of phases along the orbit, thus determining the flux variability with orbital phase. The input parameters we use in this model are listed in Table 1. We also assumed an inclination angle of 32° , as estimated by De Becker et al. (2006).

The top panel of Fig. 2 shows the resulting 6 cm radio fluxes. Clearly, this more sophisticated model is capable of providing variable non-thermal radiation, showing that at least part of the synchrotron emission can escape from the free-free absorption. The observed level of non-thermal radiation (about 1 mJy max) is not reached, but that could be due to one of the many assumptions in the model, such as the fraction of the shock energy that goes into the relativistic electrons or the magnitude of the magnetic field.

The reason that this model does predict non-thermal radiation is that the synchrotron emission region is considerably larger than expected. This may seem surprising, but it is due to the fact that at larger distances from the central line connecting the two stars a much larger volume contributes to the synchrotron emission (as the situation is rotationally symmetric around that line). That partly compensates for the fact that the synchrotron emission per volume becomes weaker as we move away from the central line. The model also predicts that in high-resolution radio images where we can resolve the colliding-wind region we will still only see the central part of the synchrotron emission

region, as the emergent intensity of the outer part will be too low for it to be detected. In this way, the model is consistent with the high-resolution radio observations (e.g. WR140, Dougherty et al. 2005).

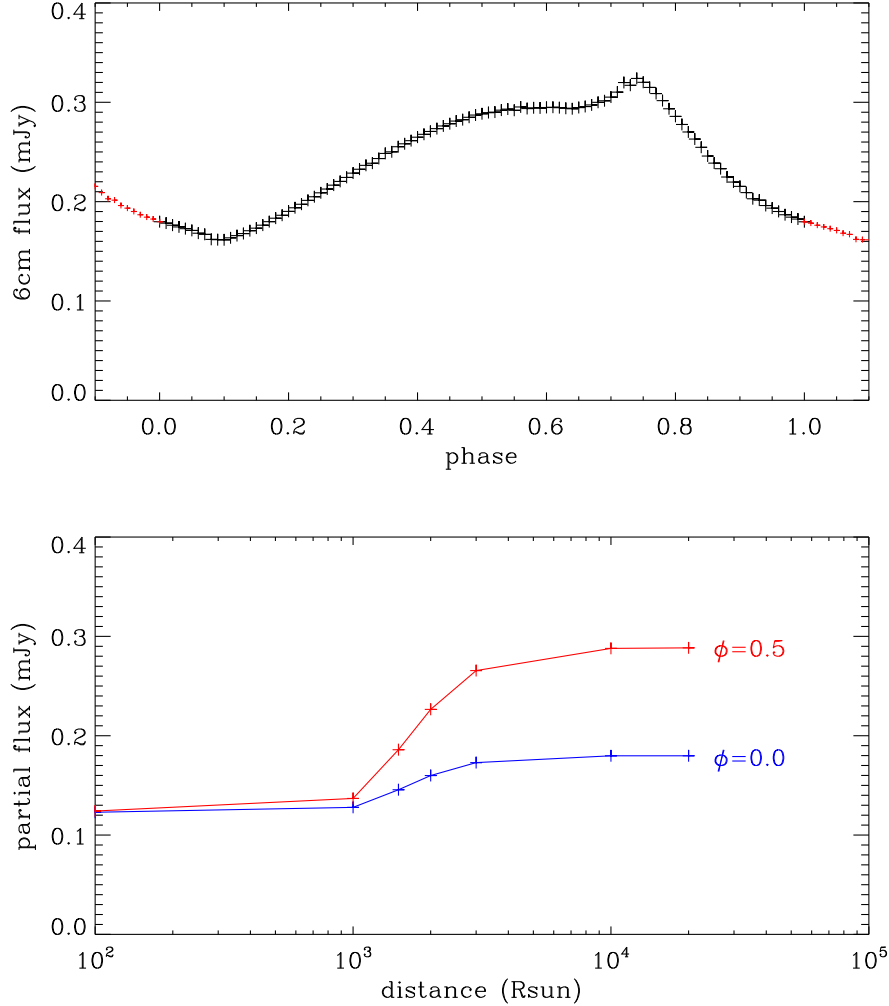


Figure 2. Results from the more sophisticated synchrotron emission model. **Top panel:** the 6 cm radio fluxes predicted by the model, as a function of orbital phase. **Bottom panel:** the cumulative flux at phases 0.0 and 0.5, as a function of distance from the central line connecting the two stars. The largest contribution of the flux occurs between 1000–3000 R_{\odot} , i.e. approximately 10 to 30 times the separation between the two stars.

We next try to quantify the extent of the non-thermal emitting region, by determining where the major part of the detected non-thermal flux comes from. We do this by numerical experiment: we artificially set the synchrotron emission to zero beyond a certain radius and see how much non-thermal radiation is still detected. The bottom part of Fig. 2 shows that with a small cut-off radius we

only obtain about 0.12 mJy, which is the free-free emission of the two stellar winds. In the region 1000–3000 R_\odot we get the main contribution, with the flux levelling off beyond that. The major flux contribution therefore comes from distances of 1000–3000 R_\odot , i.e. approximately 10 to 30 times the separation between the two stars.

Although the new model is quite successful in predicting non-thermal radiation, there is still one major problem: the phases at which maximum and minimum occur are incorrect. Observed maximum is around phase 0.1 and minimum at 0.7, but the predicted values are nearly exactly the reverse.

The parameters listed in Table 1 are based on typical values for the spectral types of both components (De Becker et al. 2006). Quite an error range is associated with these parameters, and we therefore explored if we could get a better fit to the observed data by changing some of the star and wind parameters. No exhaustive search of the parameter space was attempted, but in Fig. 3 we present an improved model, where the terminal velocity of the primary and the mass-loss rate of the secondary are increased, while the mass-loss rate of the primary is decreased. While the phase is still not correct, the difference with the observations is less. Furthermore, the general flux level is also higher and in better accordance with the observations.

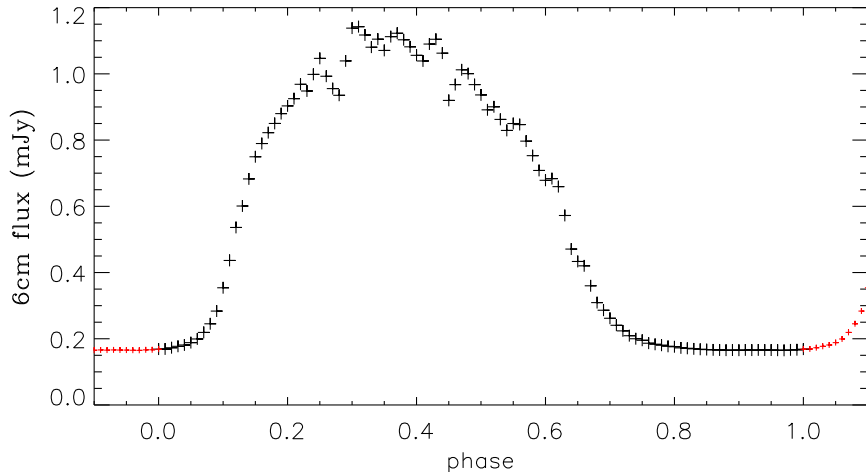


Figure 3. Predicted 6 cm radio fluxes as a function of orbital phase for a model with changed stellar parameters compared to those listed in Table 1. Here we use $v_{\infty,1} = 3500 \text{ km s}^{-1}$, $\dot{M}_1 = 2 \times 10^{-6} \text{ M}_\odot \text{ yr}^{-1}$ and $\dot{M}_2 = 6 \times 10^{-6} \text{ M}_\odot \text{ yr}^{-1}$.

To explain the remaining discrepancies, we explored a further sophistication of the model. Following the work of Parkin & Pittard (2008), we introduced the effect of orbital motion. In the simplification by Parkin & Pittard, this is done by assuming that the contact discontinuity consists of a “cap” in the inner part, which is formed instantaneously and a “ballistic” part in the outer part, where the material streams out further without any net force working on it. In the ballistic part, a “time-delay” effect needs to be taken into account: at

any given phase, the contact discontinuity in the ballistic part is the result of material emitted at the ends of the cap at some previous phase. Taking the orbital motion into account, this results in a spiral-shaped form of the contact discontinuity in the orbital plane (see Parkin & Pittard 2008, their Fig. 10).

Although the preliminary calculations presented at the meeting suggested that this would improve the agreement with the observations, we have so far not succeeded in finding a good model. As the synchrotron emission region in this model is wound up into a spiral, we detect a large part of it at any orbital phase and we therefore end up with considerably less variability as a function of orbital phase. We suspect that in the present case of Cyg OB2 No. 8A, the contact discontinuity is not as tightly wound up into a spiral as suggested by the Parkin & Pittard (2008) model. Some twisting of the contact discontinuity would undoubtedly be present, however, and this might be sufficient to explain the phase shift between the observations and simpler models.

4. Other Stars

We intend to apply the present model to a number of other binaries where we have a considerable amount of data on their non-thermal radio emission, such as HD 168112 (Blomme et al. 2005), HD 167971 (Blomme et al. 2007) and Cyg OB2 No. 9 (Van Loo et al. 2008). We will also extend the model to X-ray emission and optical spectra.

We also expect a considerable number of colliding-wind binaries to be detected in future radio surveys. One upcoming survey is COBRaS, the Cyg OB2 Radio Survey³ (PI: R.K. Prinja). This e-MERLIN legacy project has been awarded nearly 300 hrs to make a deep survey of the core of the Cyg OB2 cluster. This cluster has already provided us with three examples of colliding-wind binaries (No. 5, No. 8A and No. 9).

In our Galaxy, there are only a few examples of young, very massive clusters, of which Cyg OB2 is one. The survey will make a mosaic of the core region at 5 GHz (with a 1-sigma noise level of 3 μ Jy) and at 1.6 GHz (1-sigma noise level of 7.5 μ Jy). Its main science goals are to study (i) the mass-loss and evolution in massive stars; (ii) the formation, dynamics and content of massive OB associations; and (iii) the frequency of massive binaries and the incidence of non-thermal radiation. The combination of the two frequencies will allow us to easily distinguish the non-thermal radio emitters from the thermal ones and thereby detect the colliding-wind binaries. The high sensitivity will result in the detection of a significant number of binary systems, allowing detailed statistical studies of the colliding-wind phenomenon.

5. Conclusions

Contrary to expectations, the short-period binary Cyg OB2 No. 8A does show radio variability that is phase-locked with its 21.9-day orbital period. New models for the synchrotron emission from the colliding-wind region show that this

³<http://www.homepages.ucl.ac.uk/~ucapdwi/cobras/>

region is indeed extended enough that not all the emission is absorbed by the free-free absorption. At present, we still have the problem that the phases of minimum and maximum flux are not correctly modelled. We suspect that a combination of different wind parameters and some slight twist of the contact discontinuity due to orbital motion will be needed to explain these differences.

We note that the present model does not require any porosity in the stellar winds of both components. Colliding-wind systems such as Cyg OB2 No. 8A can therefore be highly relevant to interpreting single stars, where clumping and porosity have been proposed to explain the discrepancies in mass-loss rate determinations.

In future, the present models will be applied to other non-thermal emitters. The model will also be extended to cover X-ray and optical wavelengths. It is expected that future surveys, such as COBRaS, will turn up a considerable number of non-thermally emitting colliding-wind binaries.

Acknowledgments. We thank Joan Vandekerckhove for his help with the reduction of the VLA data.

References

- Adam, J. 1990, *A&A*, 240, 541
 Antokhin, I.I., Owocki, S.P., & Brown, J.C. 2004, *ApJ*, 611, 434
 Bell, A. R. 1978, *MNRAS*, 182, 147
 Biegging, J.H., Abbott, D.C., & Churchwell, E.B. 1989, *ApJ*, 340, 518
 Blomme, R. 2005 in *Massive Stars and High-Energy Emission in OB Associations*, ed. G. Rauw, Y. Nazé, R. Blomme, & E. Gosset, 45
 Blomme, R., Van Loo, S., De Becker, M., et al. 2005, *A&A*, 436, 1033
 Blomme, R., De Becker, M., Runacres, M. C., et al. 2007, *A&A*, 464, 701
 De Becker, M., Rauw, G., Manfroid, J. 2004, *A&A*, 424, L39
 De Becker, M., Rauw, G., Sana, H., et al. 2006, *MNRAS*, 371, 1280
 Dougherty, S.M., Beasley, A.J.; Claussen, M.J., Zauderer, B.A., Bolingbroke, N.J. 2005, *ApJ*, 623, 447
 Parkin, E.R., Pittard, J.M. 2008, *MNRAS*, 388, 1047
 Puls, J., Vink, J.S., Najarro, F. 2008, *A&ARv*, 16, 209
 Van Loo, S., Runacres, M. C., Blomme, R. 2006, *A&A*, 452, 1011
 Van Loo, S., Blomme, R., Dougherty, S.M., & Runacres, M.C. 2008, *A&A*, 483, 585